

Covalent Organic Framework Derived Carbons as Supercapacitors

A Thesis

Submitted in Partial Fulfillment of the Requirements

for the Degree of BS-MS

By

A VAMSHI KRISHNA

ID: 20141019



Indian Institute of Science Education and Research (IISER), Pune 2019

Dedicated to

My family



भारतीय विज्ञान शिक्षा एवं अनुसंधान संस्थान, पुणे
INDIAN INSTITUTE OF SCIENCE EDUCATION AND RESEARCH
(IISER), PUNE

(An Autonomous Institution, Ministry of Human Resource Development, Govt. of India)

Dr. Homi Bhabha Road, Pune – 411 008

Dr. R. Vaidhyanathan
Associate Professor

Certificate

This is to certify that this dissertation entitled “*Covalent Organic Framework derived Carbons as Supercapcitors*” toward the partial fulfillment of BS-MS dual degree programme at the Indian Institute of Science Education and Research-Pune, represents work carried out by “A VAMSHI KRISHNA” under the supervision of “Dr. R. VAIDYANATHAN, Associate Professor, Department of Chemistry” during the academic year 2018-2019.

Date: 29/03/2019
Place: Pune

Signature of student


Date: 29/03/2019
Place: Pune

Signature of Supervisor

Declaration

I hereby declare that the matter embodied in the report entitled "Covalent Organic Framework derived Carbons as Supercapcitor" are the results of the work carried out by me at the Department of Chemistry, IISER Pune, under the supervision of "Dr. R. VAIDHYANATHAN" and the same has not been submitted elsewhere for any other degree.

Date: 29/03/2019
Place: PUNE


Signature of student

Date: 29/03/2019
Place: PUNE


Signature of Supervisor

ACKNOWLEDGMENT

Firstly, I would like to express my sincere gratitude to my supervisor **Dr. R. VAIDHYANATHAN** for his continuous support, guidance, motivation and enthusiasm on science helped me successfully carried out this MS thesis. It is impossible for me to complete this work without his guidance and support. His unwavering encouragement and enthusiasm towards research kept me constantly engaged in my research and his personal generosity helped make my time enjoyable. Sir, I really enjoyed and learned a lot while working with you.

I am grateful to my thesis advisory committee member **Dr. Satish Ogale** for his guidance and helpful discussion during mid-sem presentation, which enabled me to make necessary improvements. My special thanks to former Director of IISER-Pune Prof. K. N. Ganesh and present Director Prof. Jayant B. Udgaonkar for providing excellent research facilities and an outstanding atmosphere. My sincere gratitude to all the faculty members in the IISER-Pune for teaching me various courses.

I would like to thank my astoundingly supporting lab members Dinesh, Shalini, Debanjan, Sattwick, Himan, Pragalb, Rahul, Rinku and Ankit. It was always a pleasure coming to work every day with such lovely and engaging people. My deep gratitude goes for Dinesh and Debanjan, who expertly guided me through my fifth year project and who shared happiest moments, ups, downs and joy with me. Heartfelt thanks to all my friends who made IISER Pune stay comfortable and joy able, in particular, Jayanth, Dev, Sunil, Rajat, Harsha, Satendra(IAS), Naman, Bharath, Deepraj, Parvathalu, Dharmendra, Maji, yogesh, sravan and Hrithik. Special thanks to my sister Anu Pradeep, Pranavi and Satvika for their great support especially during my fifth year. And my Special thanks to shephali dansana. Thanks everyone for their unending support.

No words can ever convey my sense of gratitude felt for my parents, brother and sister for selfless love and support throughout my career. It wouldn't have been possible for me to achieve all that without their support. It is to them that I dedicate this work. Finally, I would be signing off by thanking all of the amazing teachers who have directly or indirectly helped me along the way. Good teachers are the reason why ordinary.

TABLE OF CONTENTS

LIST OF ACRONYMS	2
LIST OF FIGURES	3
ABSTRAT	5
INTRODUCTION	6
1.1. Introduction to Covalent Organic Frameworks (COFs).....	6
1.2. Electrical Double Layer Capacitor (EDLC).....	8
1.3. Pseudocapacitor.....	9
EXPERIMENTAL METHODS	11
2.1. Synthesis of Trialdehyde Monomer.....	11
2.2. Synthesis of COF.....	11
2.3. Synthesis of Co@COF Composite.....	12
2.4. Synthesis of COF derived Carbon.....	13
2.5. Synthesis of Co@COF Derived Carbons.....	13
RESULTS AND DISCUSSION	14
3.1. Characterization of C@COF-750.....	14
3.2. Electrochemical Studies.....	17
3.2.1. Sample Preparation.....	17
3.2.2. Experimental Procedure.....	17
3.2.3. Data Analysis.....	17
3.2.4. Capacitance Calculation.....	19
3.2.5. Interpretation.....	19
3.3. Characterization of Co@COF-400 and Co@COF-750.....	20
3.4. Electrochemical Studies.....	25
3.4.1. Data Analysis of Co@COF-400.....	25
3.4.2. Data Analysis of Co@COF-750.....	26
3.4.3. Data Analysis.....	27
4.0. CONCLUSION	29
5.0. REFERENCES	30

List of Acronyms:

1	COF: Covalent Organic Frameworks	21	Å : Angstrom
2	MOF: Metal Organic Framework	22	Csp: specific capacitance
3	CP: Coordination Polymer	23	MHz: Megahertz
4	DMF: N, N-Dimethyl formamide	24	H₂SO₄: Sulphuric Acid
5	FE-SEM: Field Emission-Scanning Electron	25	V: volts
6	TGA: Thermogravimetric analysis	26	mV: Millivolts
7	PXRD: Powder X-Ray Diffraction	27	CV: Cyclic Voltammogram
8	BET: Brunauer Emmett Teller	28	M: Molar
9	GCD: Galvanostatic charge-discharge profile	29	CE: Counter Electrode
10	°C : Degree Celsius	30	WE: Working Electrode
11	mmol: Milli moles	31	RE: Reference Electrode
12	µL : Micro liter	32	A: Ampere
13	µm: micrometer	33	F: Farad
14	mL: Milliliter	34	H⁺: Hydrogen ion
15	nm : nanometer	35	mg: Milligram
16	hrs: hours	36	K: Kelvin
17	min: Minutes		
18	mol: moles		
19	gm: Gram		
20	EDLC: Electrical Double Layer Capacitance		

LIST OF FIGURES

1. INTRODUCTION

Figure 1: Design topologies of covalent organic frameworks.

Figure 2: Schematic diagram of parallel plate capacitor.

Figure 3: Schematic representation of electrical double layer capacitor.

Figure 4: Schematic representation of pseudocapacitor.

Figure 5: Schematic representation of the work carried out in this report.

2. EXPERIMENTAL METHODS

Figure 6: Schematic representation of the IISERP-COF1 synthesis and proposed topology.

3. RESULTS AND DISCUSSION

PART-1

Figure 7: Powder X-ray Diffraction pattern of the carbon showing amorphous nature of the material. (B) TGA profile showing high thermal stability. (C) Raman spectra of the carbon. (D) IR spectra of carbon.

Figure 8: SEM images of the carbon in two different magnifications.

Figure 9: (A) N₂ isotherm at 77 K. (B) NLDFT pore size distribution plot. (C) BET surface area plot. (D) Langmuir surface area.

Figure 10: (A) CO₂ adsorption isotherms at different temperatures. (B) HOA for CO₂ adsorption.

Figure 11: (A) and (B) Cyclic Voltammogram of COF derived Carbon from low to high the scan rates in 1(M) H₂SO₄ (sulphuric acid) electrolyte. (C) The linear fit of anodic peak current and cathodic peak current vs. square root of scan rate (D) Nyquist plot

Figure 12: (A) Galvanostatic charge-discharge profile of COF derived carbon at different current densities. (B) Specific Capacitance variation with the change of current densities. (C) Specific Capacitance retention after 400 cycles charge-discharge.

PART-2

Figure 13: (A) PXRD of the composites. (B) TGA of the composites showing a thermal

stability up to 400°C. (C) N₂ isotherms at 77 K. (D) NLDFT pore size distribution obtained using N₂ isotherms at 77K.

Figure 14: BET and Langmuir surface area plots for the Co@COF-400 (A, B) and Co@COF-750 (C, D).

Figure 15: IR spectra of the composites. The spectra shows that some degree of functionalities in the COF is retained on pyrolysis at 400°C, but 750°C pyrolysis produces neat carbon.

Figure 16: FESEM images of the Co@COF-400 (A, B) and Co@COF-750 (C, D) composites showing fluffy cotton like morphology.

Figure 17: Energy Dispersive X-Ray Spectroscopy (EDS) images showing significant Co atoms present in Co@COF-400.

Figure 18: Energy Dispersive X-Ray Spectroscopy (EDS) images showing significant Co atoms present in Co@COF-750.

Figure 19: (A) and (B) Cyclic Voltammogram of Co@COF-400 from low to high the scan rates in 1(M) H₂SO₄ electrolyte. **(C)** Galvanostatic Charge –Discharge profile of Co@COF-400 at different current densities. **(D)** Nyquist plot of Co@COF-400.

Figure 20: (A) and (B) Cyclic Voltammogram of Co@COF-750 from low to high the scan rates in 1(M) H₂SO₄ electrolyte. **(C)** Galvanostatic Charge–Discharge profile of Co@COF-750 at different current densities. **(D)** Nyquist plot of Co@COF-750.

Figure 21: (A) Cyclic voltammogram of Co@COF-400 and Co@COF-750 at 250 mV/s. **(B)** Galvanostatic Charge –Discharge profile of Co@COF-400 and Co@COF-750 at 250 mA/g **(C)** Specific Capacitance variation with the change of current densities of CO@COF-400 and Co@COF-750. **(D)** Linear Fit of Anodic Peak and Cathodic Peak Current Vs Square Root of Scan Rate of Co@COF-400 and Co@COF-750. **(E)** Specific Capacitance retention after 1000 cycles Charge-discharge.

ABSTRACT

Covalent organic frameworks (COFs) are a new class of porous materials which are basically crystalline organic porous polymers¹. In the last decade, COFs have been studied intensively for its diverse chemical nature and applications². COFs have been prepared to employ different chemistries like boronic ester formation, Schiff base formation, hydrazine bond formation, benzimidazole bond formation etc. Among them, Schiff base COFs are well explored because of its diverse number of building block library available³. COFs have found potential applications in gas storage⁴, separation⁵, heterogeneous catalysis⁶, energy storage⁷ etc. Still, COFs suffer stability and conductivity issues in different applications⁸. Recently, very few COFs are burnt to generate porous carbons⁹. Porous carbons from COFs would have few advantages over carbon generated from other precursors. First of all, COFs due to its ordered structure would generate ordered crystalline heteroatom doped carbon¹⁰, which will have more effect on the structure-property relationship. Secondly, the conductivity of the material can be increased by controlled carbonization. COFs are a very bad conductor of electricity. But on carbonization, the conductivity issue can be resolved and the final carbon can bring improved performance for different electrochemical applications¹¹. Still, there are disadvantages of COF-derived carbons in terms of specific applications like carbon capture. The carbon doesn't have good selectivity of CO₂ over N₂. Despite the advantages and disadvantages COF-derived carbon are now widely used for different applications like energy storage, electrochemical water oxidation and reduction etc.

1. INTRODUCTION

1.1. Introduction to covalent organic frameworks (COFs)

Covalent organic frameworks (COFs) are new class of porous materials which are basically crystalline organic porous polymers¹. In last decade, COFs have been studied intensively for its diverse chemical nature and applications². COFs have been prepared employing different chemistries like boronic ester formation, Schiff base formation, hydrazine bond formation, benzimidazole bond formation etc. Among them Schiff base COFs are well explored because its diverse number of building block library available³. COFs have found potential application in gas storage⁴, separation⁵, heterogeneous catalysis⁶, energy storage⁷ etc. Still COFs suffer stability and conductivity issues in different applications⁸. Recently, very few COFs are burnt to generate porous carbons⁹.

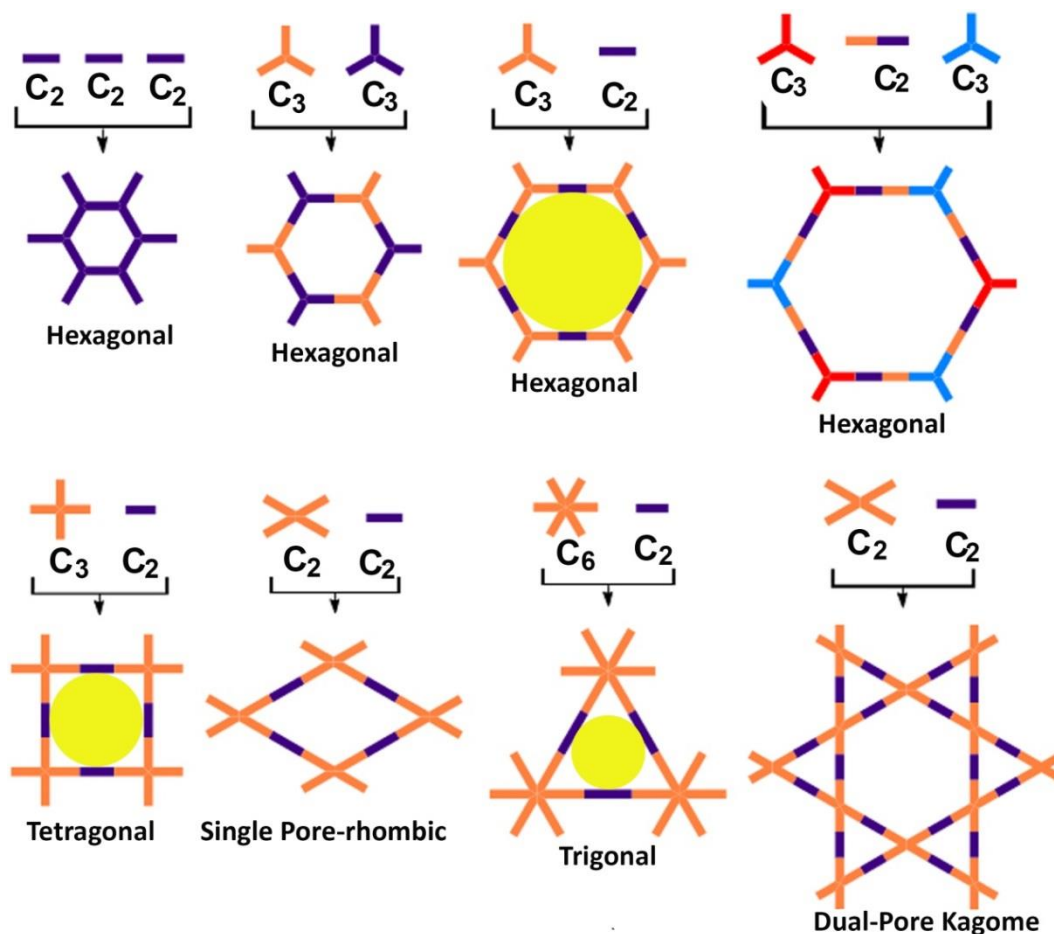


Figure 1: Design topologies of Covalent Organic Frameworks.

Porous carbons from COFs would have few advantages over carbon generated from other precursors. First of all, COFs due to its ordered structure would generate ordered crystalline hetero atom doped carbon¹⁰, which will have more effect on structure property relationship. Secondly, the conductivity of the material can be increased by controlled carbonization. COFs are themselves are very bad conductor of electricity. But on carbonization the conductivity issue can be resolved and the final carbon can bring improved performance for different electro chemical applications¹¹. Still there are disadvantages of COF-derived carbons in terms of specific application like carbon capture. The carbon doesn't have good selectivity of CO₂ over N₂. Despite of the advantages and disadvantages COF-derived carbon are now widely used for different applications like energy storage, electro chemical water oxidation and reduction etc.

The last few decades of drastic urbanization and industrialization have led to a unrestricted and progressive increase in the utilization of natural resources for the generation of energy (such as coal and mineral). This could lead to the exhaustion earth's nature resources and increase in global warming in forthcoming centuries. These two major problems have motivated the scientists to explore the alternative energy resources of clean, green and sustainable energy (such as wind and solar energy) and whenever needed they can obtain the desirable amount electricity¹². Over the decades, different energy resources have be made (such as supercapacitors, batteries etc). These two energy resources are used the most because of their high energy storage capacity and they have different methods of storing energy. Batteries have a low power density and lose the ability to retain the energy because the charge and discharge process is slow in batteries and over time there are degradations of chemical compounds inside the battery. But supercapacitors have high power density and high storage capacity over the time of these features it is more used as energy storage resource.

Supercapacitors are energy storage device which has high capacitance values than other capacitors. It can store 10 to 100 times more energy per unit volume or mass than a electrolytic capacitor. Capacitor stores energy by separating charge to induce a voltage in a parallel plates capacitor this is done by charging opposing plates separated

by dielectric. Unlike batteries no chemical reaction occurs during operation so life time of capacitors is more than batteries.

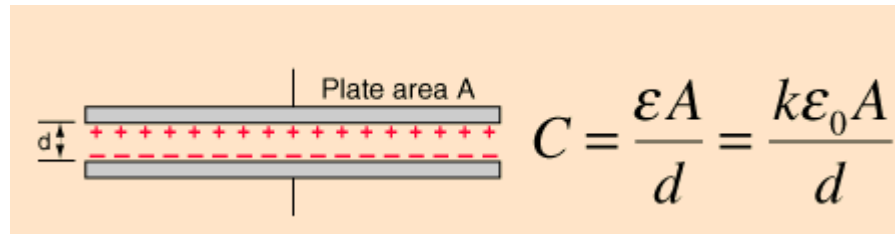


Figure 2: Schematic diagram of parallel plate capacitor.

Supercapacitors have an electrolyte between the plates rather than a dielectric. In this they use carbon electrodes so charged by formation of electrical double layers. Double layers are formed when the ions in electrolyte are attracted to an oppositely charged electrode when an electric field is induced across the device. The double layer consists of two layers one is Helmholtz layer another is diffuse layer. Helmholtz layer is made up of a dense layer of ions separated from an oppositely charged electrode by a layer of solvent molecules. The diffuse layer consists of ions diffusing to the Helmholtz layer boundary. The Helmholtz layer dominates the capacitance and can be thought of as a parallel plate capacitor where d is the thickness of the solvent layer. The thickness (d) is very small for the supercapacitors. That's why supercapacitors have more capacitance than normal capacitors. Supercapacitors are divided into two types Electrical Double Layer Capacitor (EDLC) and pseudocapacitor.

1.2. Electrical Double Layer Capacitor (EDLC)

Electrical Double Layer Capacitor (EDLC) stores charge electrostatically (Helmholtz layer). In EDLC, the double layer which is formed in between the electrodes and electrolyte. Capacitance is directly proportional to the surface area of the double layer. That's why they use the high surface area materials as electrodes to have high capacitance.

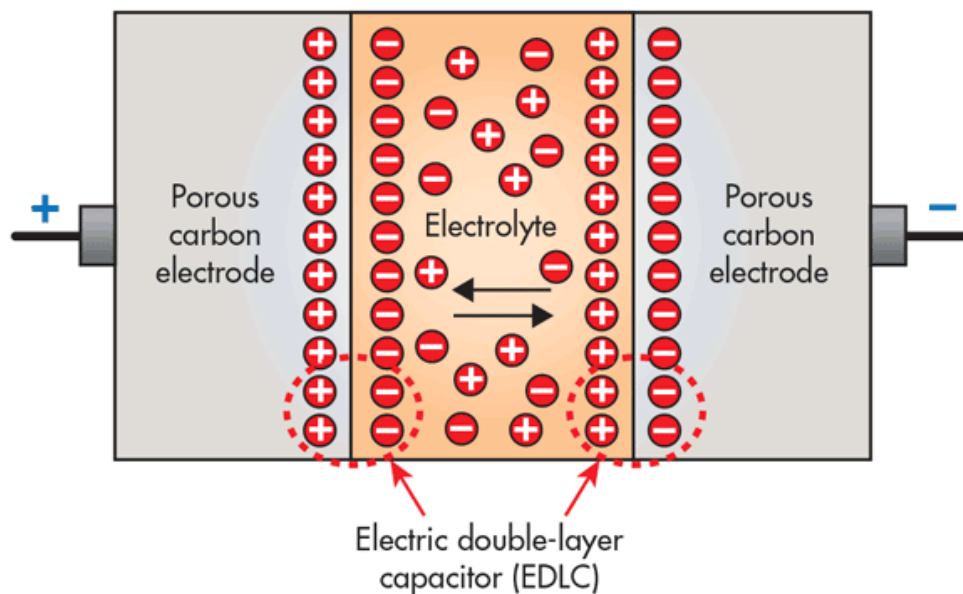


Figure 3: Schematic representation of Electrical Double Layer Capacitor.

1.3. Pseudocapacitor

Pseudocapacitors store charge electrochemically (Faradically). In pseudocapacitors, there is formation of the double layer and also there is a chemical reaction between the electrode and the ions. In EDLCs, there is formation of a double layer electrostatically with no interaction of ions with the electrode. In a pseudocapacitor, at one electrode, reduction takes place and at the other electrode, oxidation happens. During discharge, the reactions will be reversed. A pseudocapacitor has 100 times more capacitance than the EDLC with the same electrode surface.

From the last few years, scientists are trying to improve the energy storage device. To improve the performance of the energy storage device, they require a functionalized porous material with a high surface area and hierarchical porosity. Scientists have done so many experiments to improve the performance of the energy storage device on activated porous carbons, metal oxides, graphene, conjugated microporous polymers, various carbon materials, etc. Among all nanoporous materials, covalent organic frameworks (COFs) are a very different class of organic materials because of their mechanical durability, high surface area, porosity, crystalline nature, low density, and their topographies are tunable and adjustable¹².

Pseudocapacitance with specifically adsorbed ions

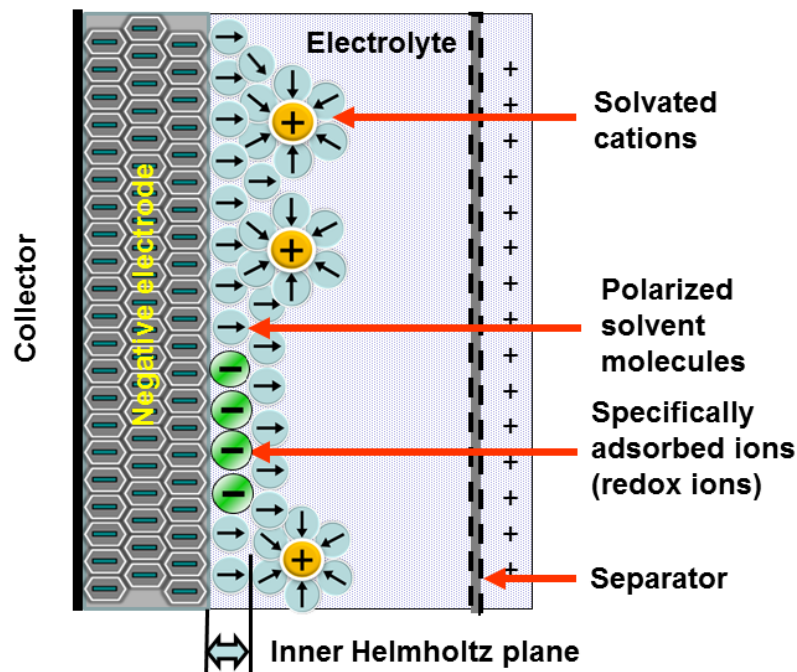


Figure 4: Schematic representation of Pseudocapacitor.

COF derived carbon can serve as a promising candidate for supercapacitors. Being highly porous, they provide a matrix for generation of porous carbon with retention of crystallinity and ease of ordered hetero atoms. Also they can host small sized nano particles like metal, oxide, nitride etc. depending upon the synthetic condition. For example, Cobalt and its oxides are widely studied for supercapacitor application. Porous cobalt oxides with tunable hierarchical morphologies for supercapacitor electrodes¹³. If COF derived carbon is doped with such kind of metal or metal oxide nano particles, this may reveal some important feature of the application. In this work we opted two methodologies. In Part-I we have investigated the CO₂ adsorption and supercapacitive property of a COF-derived carbon. Part-II contains the supercapacitor performances of two composites which are prepared by doping Co nano particles into the COF and pyrolysing the COF at two different temperatures (Figure 5).

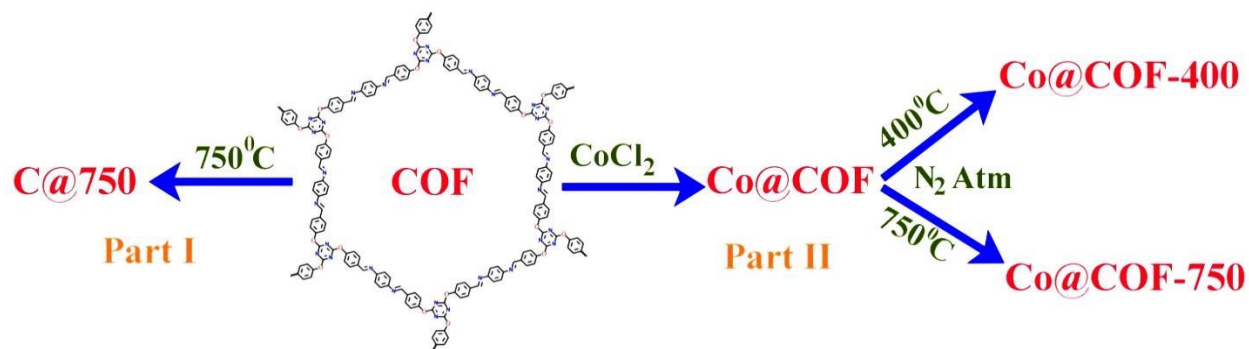
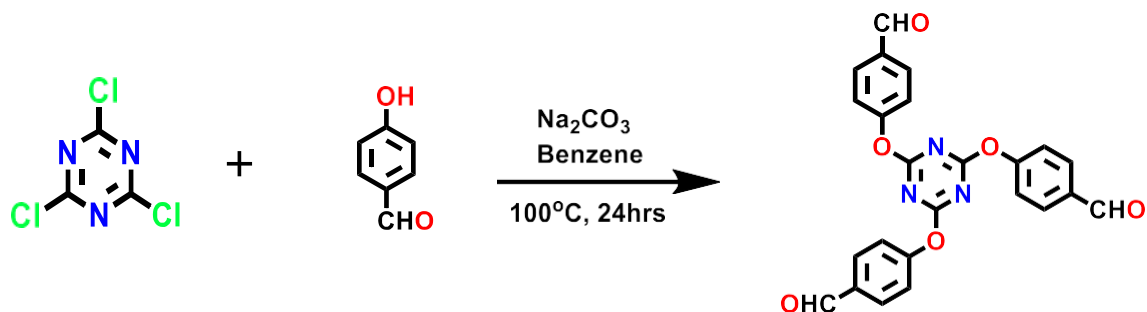


Figure 5: Schematic representation of the work carried out in this report.

2. EXPERIMENTAL METHODS

2.1. Synthesis of Trialdehyde Monomer



1.5 g of Cyanuric chloride and 4g of p-hydroxybenzaldehyde were added to a suspension of Na_2CO_3 (30 g) in 150 mL of benzene¹⁴. The resulting mixture was refluxed at 100°C for 24 hrs. After 24hrs, the hot reaction mixture was filtered and washed with an excess of hot ethylacetate and filtrate was extracted with 10% Na_2CO_3 . The subsequent organic layer was dried with anhydrous Na_2SO_4 and evaporated using rota evaporator to obtain a white powder of the desired compound (72%). The product was characterized using NMR, HRMS and the characterization results were found to be are consistent with the literature reports. All p-Phenylenediamine and organic chemicals were purchased from Sigma Aldrich and used without any further purification.

2.2. Synthesis of COF

2,4,6-Tris(p-formylphenoxy)-1,3,5-triazine (TRIPOD aldehyde) (100 mg, 0.23mmol) 1,4- diaminobenzene (48 mg, 0.46mmol) were dissolved in 1,4-dioxane (5.0

mL) in a Pyrex tube¹⁴. To this mixture, mesitylene (5.0mL) was added and the contents were homogenized by stirring. Following this, about 0.5 mL of 3M aqueous acetic acid was added. Then the Pyrex tube was flash-frozen in a liquid nitrogen bath, the free space was evacuated and the tube was closed under a blanket of nitrogen. The tube was placed in an oven at 120 °C for 3 days. A brown solid was obtained, which was washed with DMF, dioxane, acetone and THF to remove any unreacted monomers or oligomers. The reaction yielded 110 mg (87%) of IISERP-COF1. Activation of the sample for gas adsorption was done by soaking the sample in THF for 3days with three time replenishment of the solvent. (CHN Analysis: Observed. C = 66.9; H = 3.74; N = 17.38. Calculated. 70.9; H = 5.41; N = 15.04, (Note: the CHN values have been calculated using a COF unit constructed with a trialdehyde monomer and phenylenediamine with a ratio of 2:3.

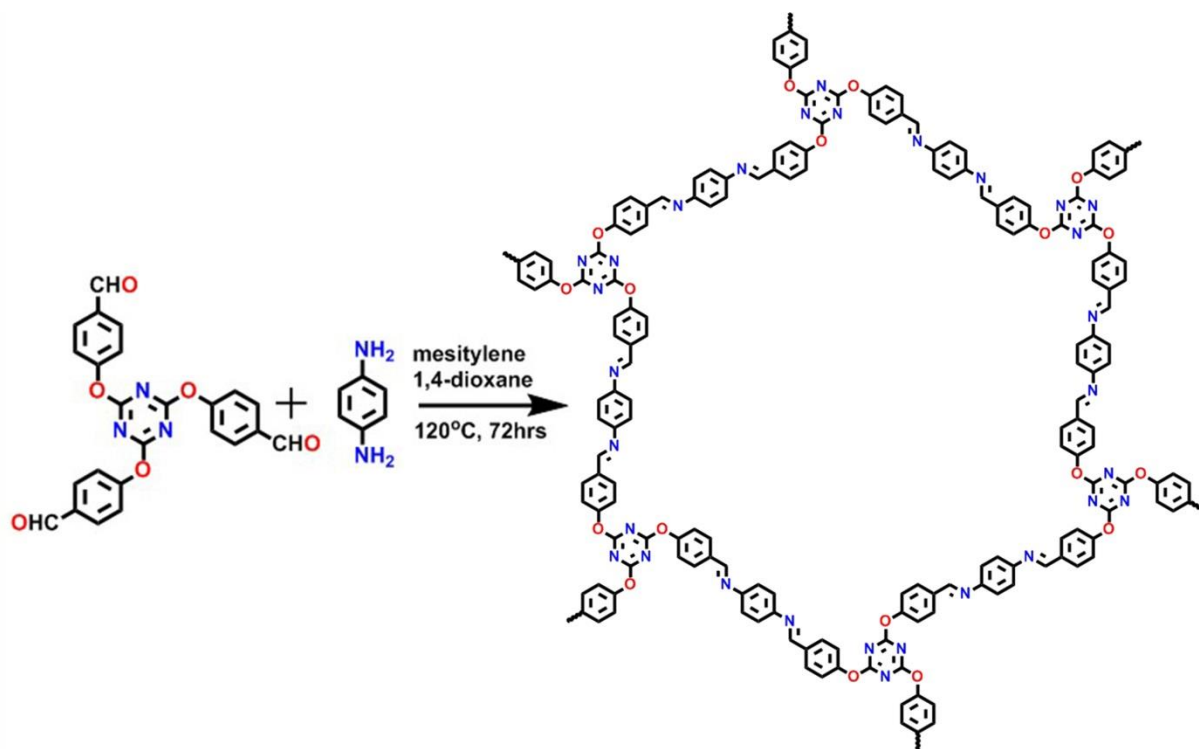


Figure 6: Schematic representation of the COF synthesis and proposed topology.

2.3. Synthesis of Co@COF composite

In a typical synthesis, the COF (100 mg) was dispersed in 40mL of n- hexane and the mixture was sonicated for about 30 min resulting in a red color dispersion¹⁵. To

this, a clear methanolic solution of $\text{CoCl}_2 \cdot 6\text{H}_2\text{O}$ (100 mg in 0.2 mL of MeOH) was added drop by drop over a period of 3h with vigorous stirring. Contents were stirred for 12h at room temperature. The solid particles are extracted by decanting the solvent and were dried at room temperature. The solid was heated at 150°C for 12h and then cooled to room temperature. This solid was suspended in 20 mL of water and the reduction was carried out by adding 30 mL freshly prepared 0.6 M aqueous NaBH_4 solution under vigorous stirring. This resulting solid was washed with copious amounts of millipore water and ethanol. These results in the formation of the COF supported cobalt catalysts as a redish-brown color solid. The synthesized samples were collected by centrifuging and dried under vacuum then used for the characterizations and catalytic studies. Also, the final redish-brown solid even upon sonicating in water did not seem to produce any colored solution, suggesting the lack of any unreacted or unloaded Co^{2+} salts that could be leaching out.

2.4. Synthesis of COF Derived Carbon

The most widely employed technique to synthesize carbon is the pyrolysis. The COF is grinded thoroughly and taken in quartz crucible. And it is burned in inert atmosphere (such as N_2 and Argon) at 750°C for 4 hrs. Pyrolysis the COF in the tube furnace resulted in black mass of porous carbon.

2.5. Synthesis of Co@COF Derived Carbons

Synthesis of carbon derived from the Co@COF is same as synthesis of carbon derived from COF. In this we synthesis two carbons one is Co@COF 750 (pyrolysis at 750°C and another one is Co@COF 400 (pyrolysis at 400°C). The Co@COF is taken in quartz crucible and it is burned at high temperatures (such as 750°C and 400°C) in inert atmosphere for 4 hrs. Pyrolysis the Co@COF in the tube furnace resulted in carbons.

PART -1

3. RESULTS AND DISCUSSION

3.1. CHARACTERIZATION OF C@COF-750

The formation of the carbon was confirmed from the Powder X-ray Diffraction (PXRD) pattern of the material. In the PXRD it appears as a broad hump, whereas the peaks for the COF are absent. This clearly indicates the complete carbonization of the COF (Figure 7A). The Thermo Gravimetric Analysis (TGA) shows that the carbon material is stable up to 500°C (Figure 7B). The Raman spectrum of the material prominently shows the presence of D band and G band (Figure 7C). D band appears at 1352 cm^{-1} and G band appears at 1577 cm^{-1} . D band corresponds to the defects present in the carbon and G band signifies the graphitic nature of the carbon. Finally, the Infra-Red spectrum shows presence of characteristics peaks for the C=C, C-C bond stretching and bending vibrations Figure (7D).

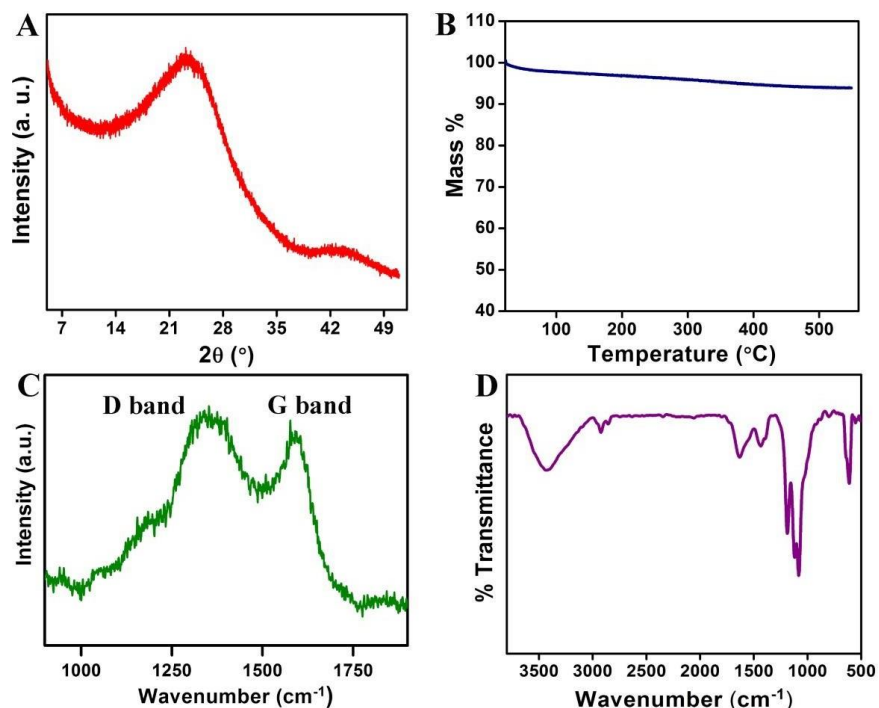


Figure 7: (A) Powder X-ray Diffraction pattern of the carbon showing amorphous nature of the material. (B) TGA profile showing high thermal stability. (C) Raman spectra of the carbon. (D) IR spectra of carbon.

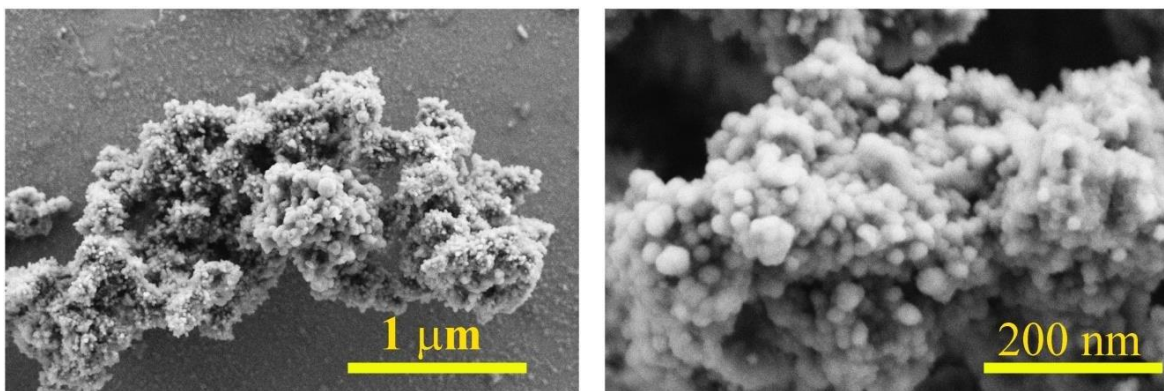


Figure 8: SEM images of the carbon in two different magnifications

To obtain the morphology of the carbon Scanning Electron Microscopy (SEM) was performed. The carbon possesses spherical morphology evidenced from SEM images (Figure 8).

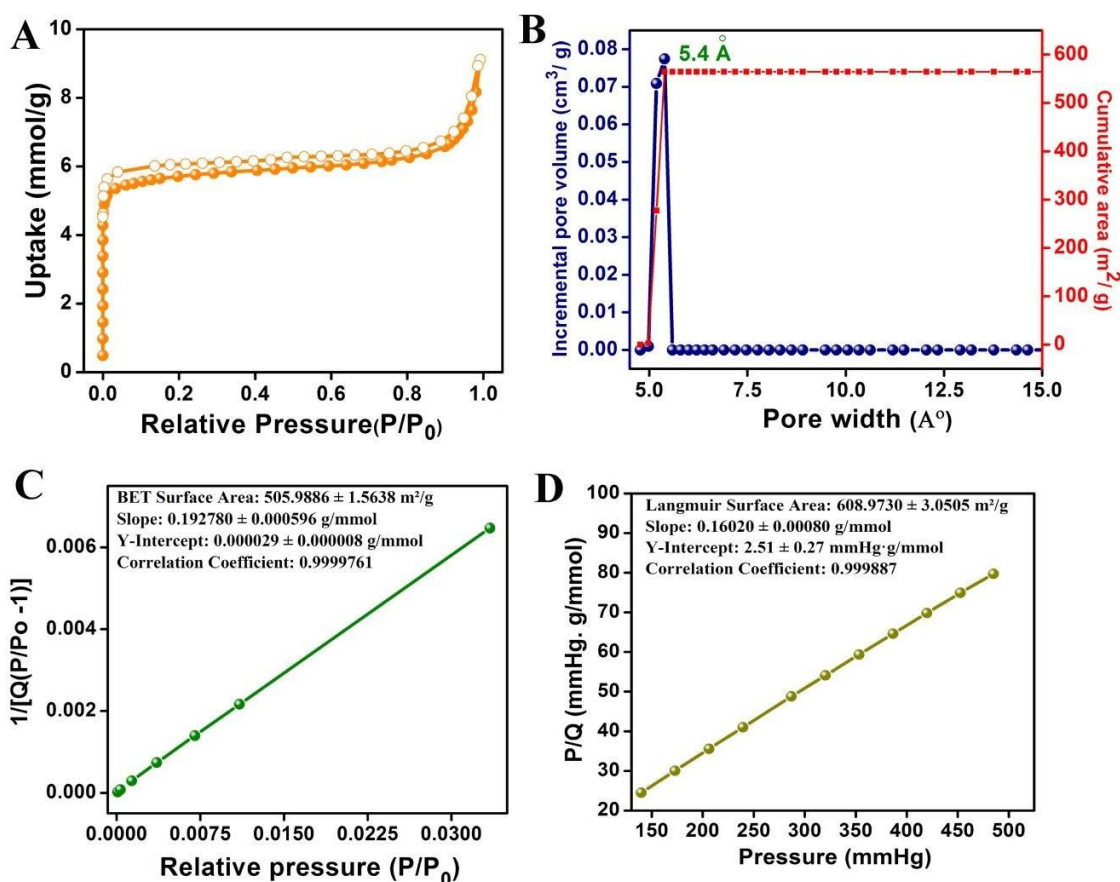


Figure 9: (A) N_2 isotherm at 77 K. (B) NLDFT pore size distribution plot. (C) BET surface area plot. (D) Langmuir surface area.

To check the porosity of the carbon, N₂ 77 K adsorption was performed. (Figure 3A shows) the N₂ at 77 K isotherm profile. It is Type-I isotherm with sharp uptake of N₂ at low pressure. Interestingly, the pyrolysis of the COF at 750°C yields a truly micro porous carbon with a pore size of 5.4 Å. The NLDFT fit from the isotherm gives a single micro pore of 5.4 Å (Figure 9B). The carbon possesses a substantially high surface area. Fitting the BET and Langmuir equations the surface area of the carbon is obtained as 505 and 608 m²/g respectively. This high surface area makes the carbon a suitable candidate for applications such as carbon capture and energy storage.

Further to check its ability to capture CO₂, isotherm measurements were performed at four different temperatures. The carbon shows reasonable CO₂ uptake at room temperature (~2.3 mmol/g) and a saturation uptake (~7.4 mmol/g) (Figure 10B). The Heat of Adsorption (HOA) was calculated with Virial model using Clausius-Clapeyron equation. The zero loading HOA is obtained ~14 kJ/mol (Figure 10B). The HOA value is quite low for the carbon. This is due to unavailability of basic sites or chemical functionality in the carbon matrix which is observed in case of MOFs, porous polymers etc.

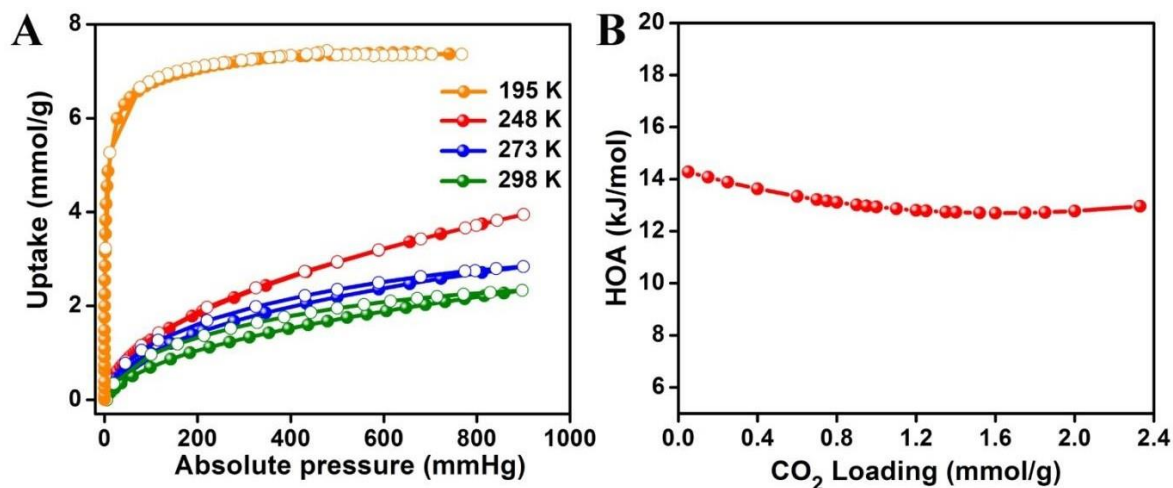


Figure 10: (A) CO₂ adsorption isotherms at different temperatures. (B) HOA for CO₂ adsorption.

3.2. ELECTROCHEMICAL STUDIES

3.2.1. Sample preparation

Due to less conducting nature of the COF derived carbon a slurry was prepared by using 60% of COF derived carbon, 30% of Super-P carbon, 10% PVDF binder in NMP solution. 2 μL of that mixture solution was drop casted on Glassy-carbon working electrode and was dried in vacuum oven at 80°C for 12 hrs. 2 μL of that slurry contained 8 μg of the of the COF derived carbon.

3.2.2. Experimental procedure

Cyclic Voltammetry (CV) measurements were performed in a conventional three-electrode system (where as working electrode (WE): COF derived carbon coated Glassy carbon, reference electrode (RE): Saturated calomel electrode, counter electrode (CE): Platinum wire and as electrolyte 1(M) H_2SO_4 were used). CVs at different scan rate from 5 mV to 1000 mV in different potential window had taken to verify is there any capacitance behavior present or not (Figure 11A and 11B).

3.2.3. Data analysis

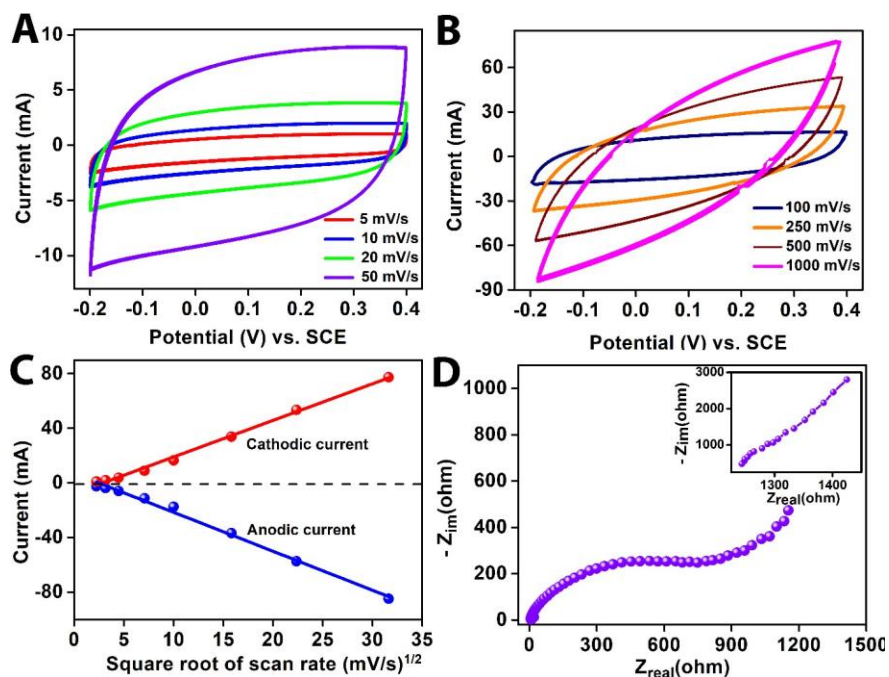


Figure 11: (A) and (B) Cyclic Voltammogram of COF derived Carbon from low to high the scan rates in 1(M) H_2SO_4 (sulphuric acid) electrolyte. (C) The linear fit of anodic peak current and

cathodic peak current vs. square root of scan rate **(D)** Nyquist plot shows the resistance of the material for charge transport. (Inset) Bulk diffusion region of the impedance plot in very low frequency region.

A rectangular type CV without any redox active peak was obtained at lower scan rates from 5 to 50 mV within the potential window from -0.2 to 0.4 V (Figure 11A). This indicates the potential of this COF derived carbon material to use as supercapacitor in acidic medium. However, with the increase of the scan rate the regular rectangular shape deforms. That may be due to the material's inability to store the H⁺ ion during its fast movement (Figure 11B). The mechanism of charge storage can be due to either charge transfer or mass transfer or both. This can be established from a plot of the peak current vs. square root of the scan rate. The cathodic and anodic peak current of COF derived carbon increases linearly with square root of scan rate demonstrating that the fast kinetics associated with H⁺ ion diffusion in the bulk materials (Figure 11C) Potentiostatic impedance analysis in this three-electrode system shows a very high charge transfer resistance of 600 ohms along with a linear bulk diffusion region (Figure 11D). Charge-discharge measurements at variable current densities were carried out to estimate the Capacitance value of the COF derived carbon material (Figure 12A).

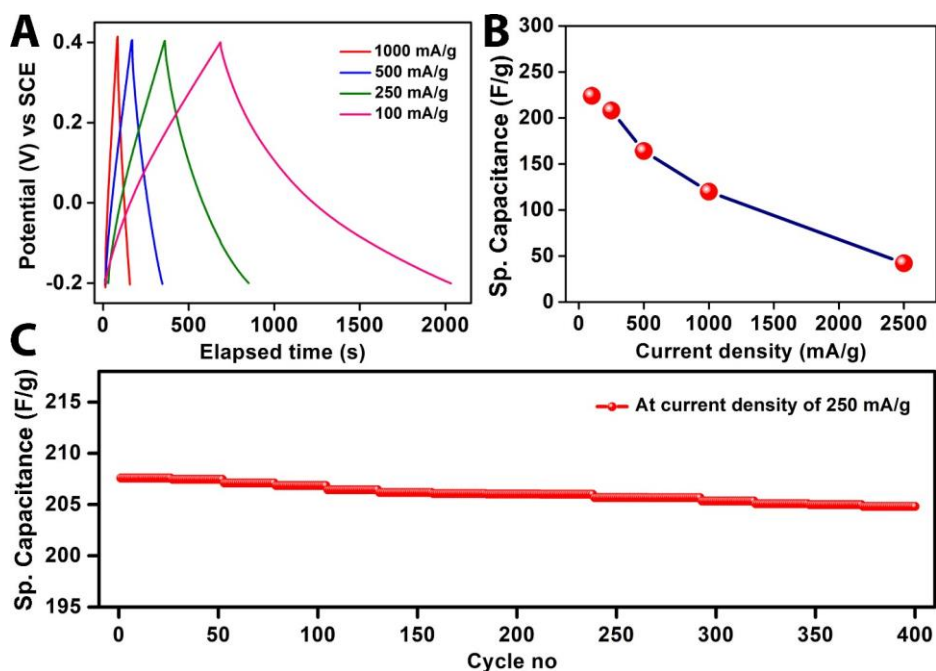


Figure 12: (A) Galvanostatic charge-discharge profile of COF derived carbon at different

current densities. **(B)** Specific Capacitance variation with the change of current densities. **(C)** Specific Capacitance retention after 400 cycles charge-discharge.

3.2.4. Capacitance calculation

The specific capacitance (C_{sp}) was derived from the GCD curve using the below equation.

$$C = (I \times \Delta t) / (\Delta V \times m)$$

Where I is the applied current density, Δt is the discharge time, ΔV is the potential window and m is the weight of electrode material. The GCD charge-discharge profiles appeared as equilateral triangle shapes, implied EDLC behavior and ideal charge storage activity with a good reversibility of the electrode material through the charge-discharge. In all the cases, Charging and discharging time are almost same (Figure 12A). The highest specific capacitance was estimated 224 F/g at 100 mA/ g current density. Which drops-down drastically with the increase of the current density (Figure 12B). However, 99% capacitance retention was achieved at 250 mA/g current density even after 400 cycles charging- discharging (Figure 12C).

3.2.5. Interpretation

The very high charge transfer resistivity and this drastic falling down of the Specific capacitance at higher current densities suggest that there are a lot of room to improve the conductivity of the COF derived carbon. Therefore, it can hold the H^+ ions even in high load of current.

PART-2

3.3. CHARACTERIZATION OF Co@COF-400 and 750

The Co loaded COF was subjected to two different pyrolysis temperature and the formation of the Co loaded carbon was characterized with Powder X-Ray Diffraction (PXRD), Thermogravimetric Analysis (TGA), N₂ 77 K isotherms, Infra-Red spectroscopy (IR) etc. Two temperatures have been chosen, 400°C and 750°C. Comparing the TGA of the parent COF, We have decided the pyrolysis temperature. The formation of the carbon composite was confirmed by PXRD (Figure 13A).

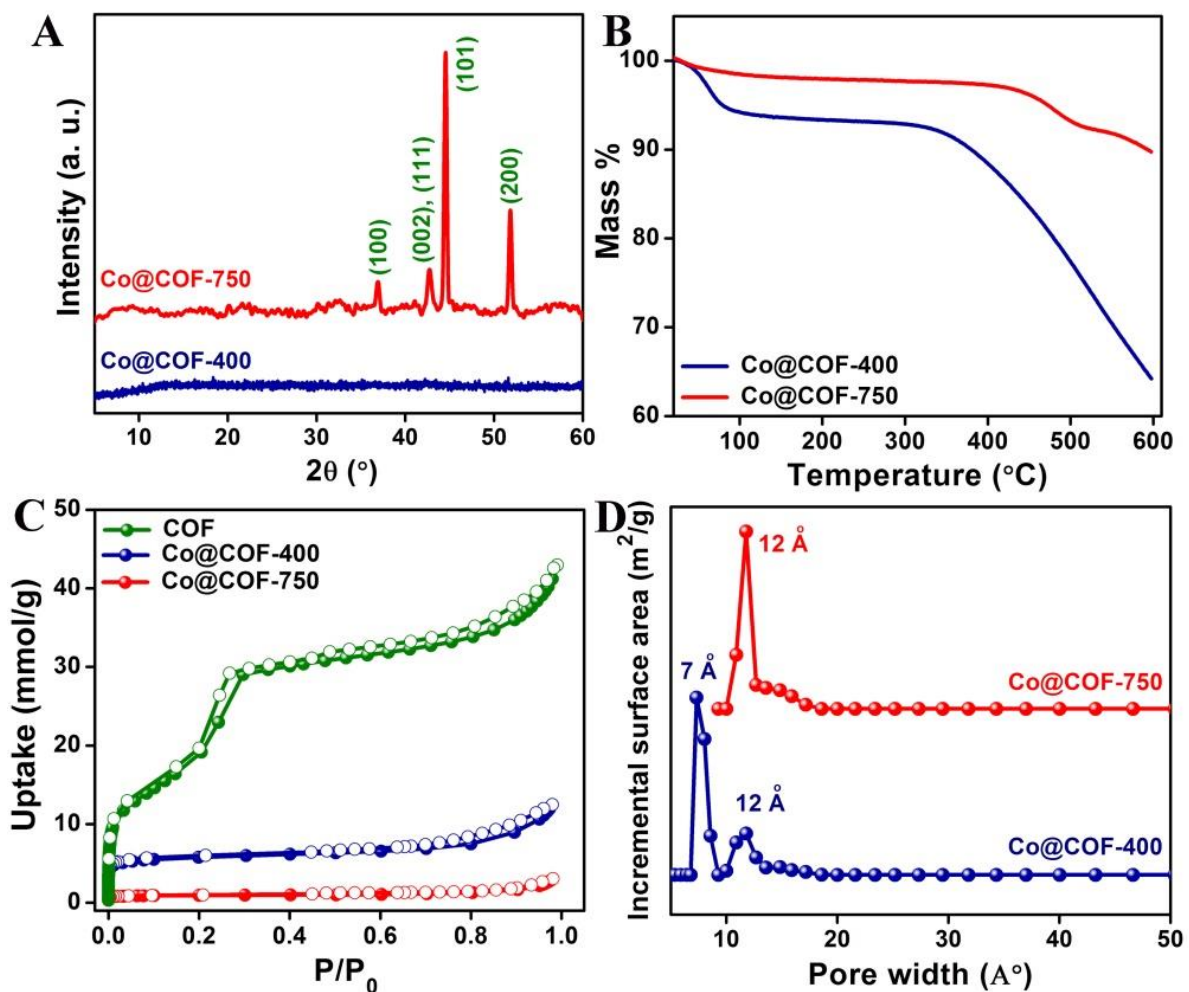


Figure 13: (A) PXRD of the composites. (B) TGA of the composites showing a thermal stability up to 400°C. (C) N₂ isotherms at 77 K. (D) NLDFT pore size distribution obtained using N₂ isotherms at 77K.

In PXRD of the pyrolysed composite at 400°C, there are no peaks for the Co nano particles. But the composite pyrolysed at 750°C contains sharp peaks of Co nano particles (corresponding planes are index to Co (nanoparticle) np, (JCPDS 05-0727). Comparing the PXRD, it has been revealed that the Co particles grow bigger with increasing the pyrolysis temperature. TGA curves of the composite show that both of them are thermally stable up to 400°C (Figure 13B). In order to evaluate the surface area, we have performed the N₂ isotherm at 77K. Figure 1C shows that there is considerable loss in nitrogen uptake which indicates that the Co nano particles are embedded into the pore of the COF. Co@COF-750 has very less N₂ uptake because the particles are grown bigger as the temperature is being increased. The pore size of the composites was evaluated from Non Local Density Functional Theory (NLDFT) fit. It has been found that both of the composites have microporous structure, with a pore dimension ranging from 7 to 12 Å (Figure 13D). But none of them possess hierarchical pores.

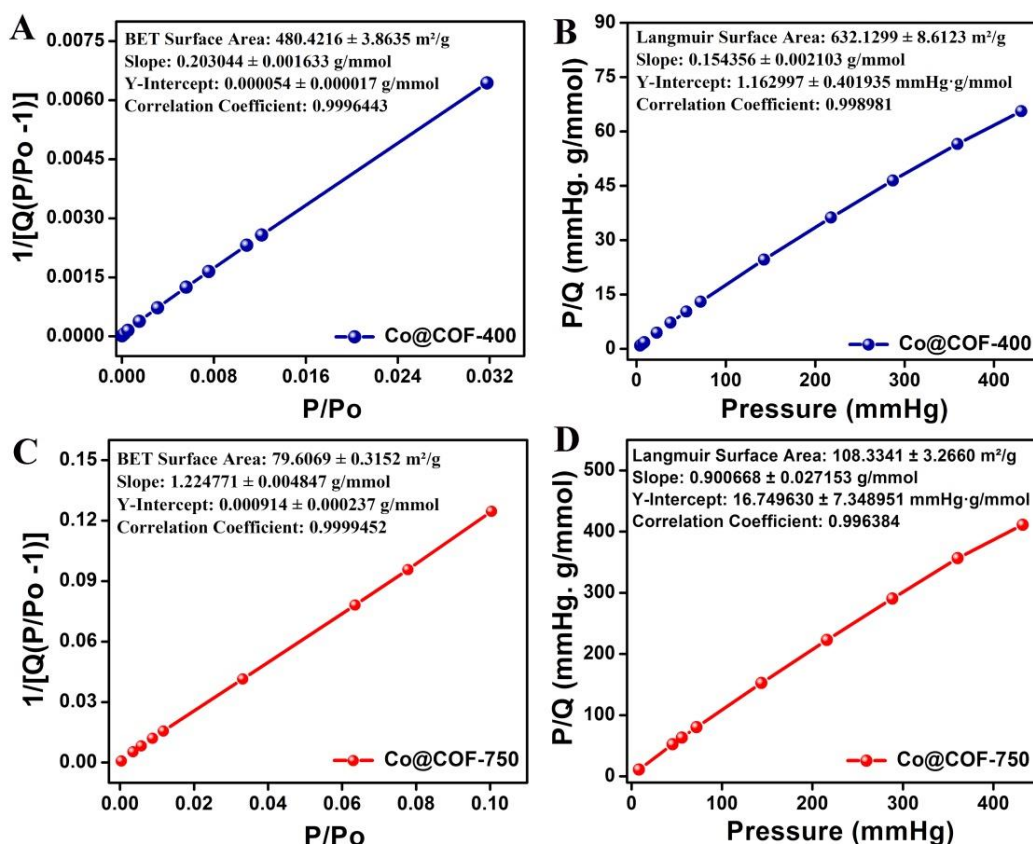


Figure 14: BET and Langmuir surface area plots for the Co@COF-400 (A and B) and Co@COF-750 (C and D).

Brunauer–Emmett–Teller (BET) and Langmuir surface areas have been obtained from the N₂ data recorded at 77 K. It has been found that Co@COF-400 has greater surface area than Co@COF-750. This observation corroborates by the PXRD results as the Co nano particle size is bigger for Co@COF-750 than the other. The IR spectra shows that some degree of functionalities in the COF is retained on pyrolysis at 400°C, but 750°C pyrolysis produces neat carbon. This has a significant implication on the nano particle sizes (Figure 15).

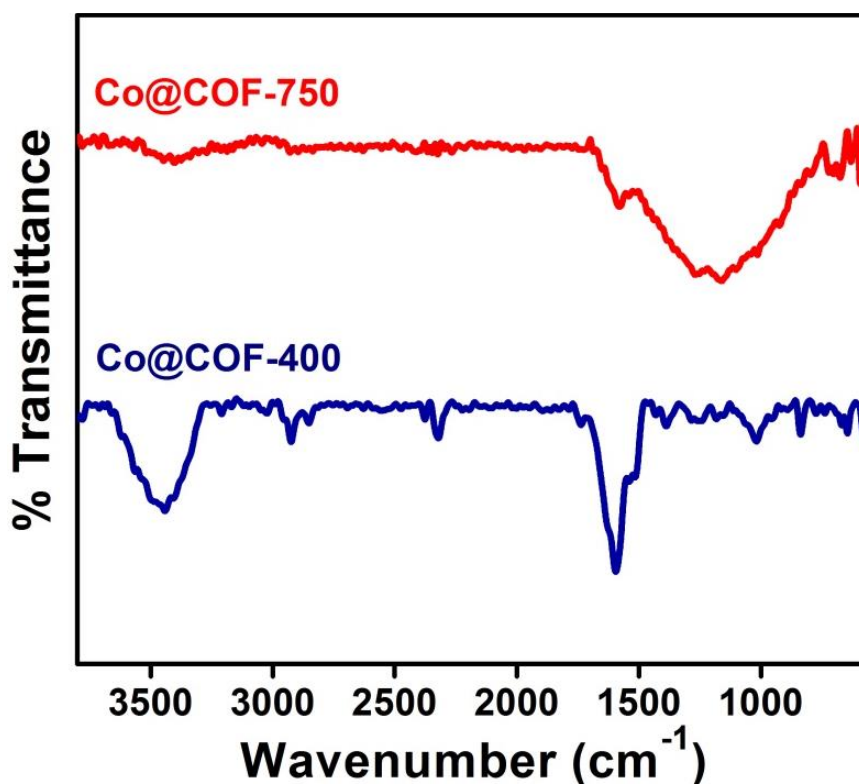


Figure 15: IR spectra of the composites. The spectra show that some degree of functionalities in the COF is retained on pyrolysis at 400°C, but 750°C pyrolysis produces neat carbon.

The morphology of the composites was obtained from Field Emission Scanning Electron Microscopic (FESEM) images. The carbon composites have fluffy cotton like morphology which is made of small spheres (Figure 16).

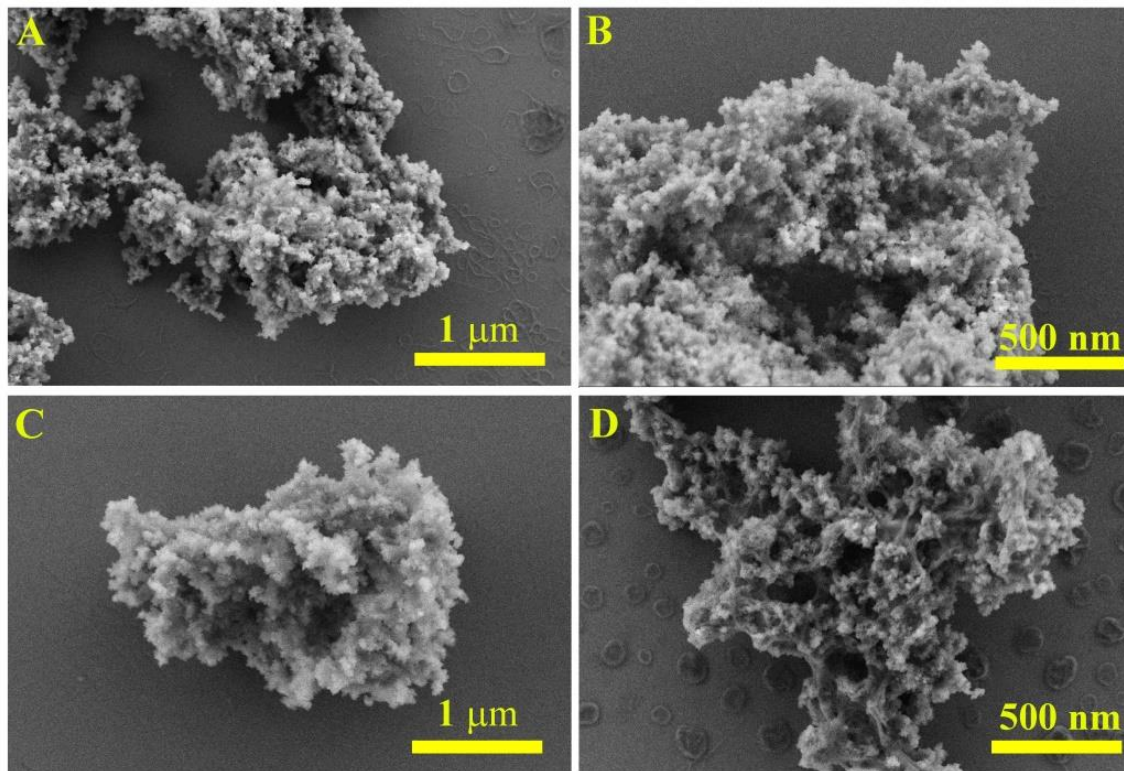


Figure 16: FE-SEM images of the Co@COF-400 (A, B) and Co@COF-750 (C, D) composites showing fluffy cotton like morphology.

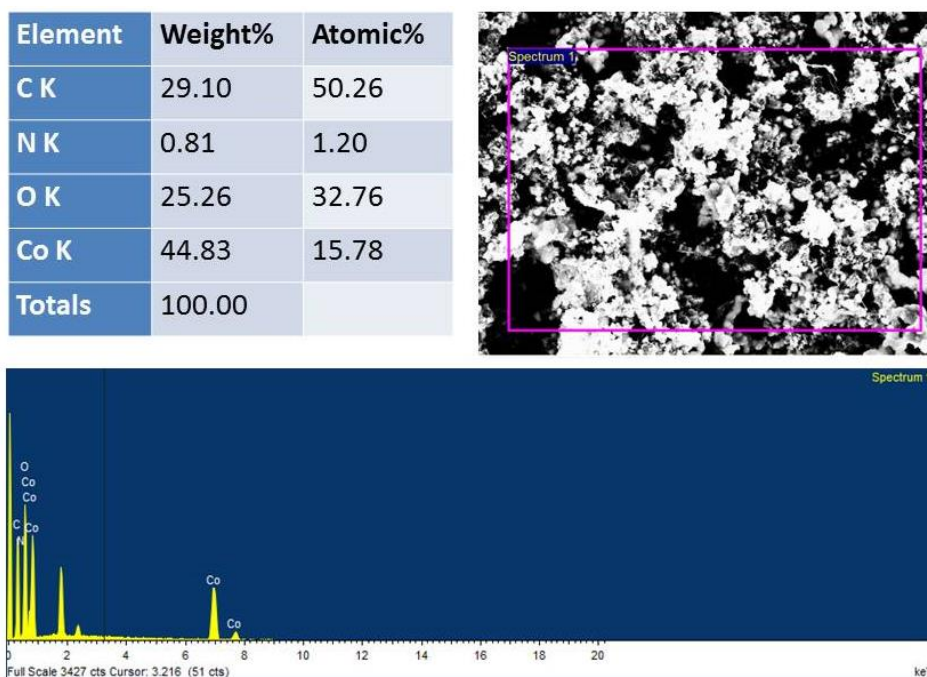


Figure 17: Energy Dispersive X-Ray Spectroscopy (EDS) images showing significant Co atoms present in Co@COF-400.

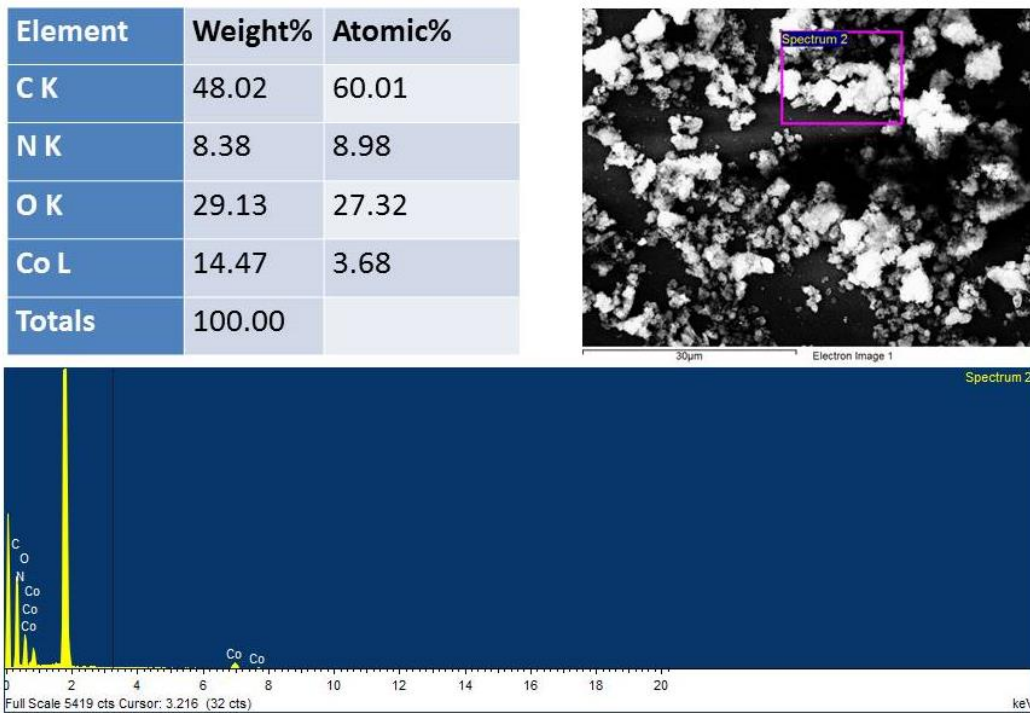


Figure 18: Energy Dispersive X-Ray Spectroscopy (EDS) images showing significant Co atoms present in Co@COF-750.

3.4. ELECTROCHEMICAL STUDIES

The sample preparation, experimental procedure for electrochemical measurements and specific Capacitance calculations of Co@COF-400 and Co@COF-750 are same as Carbon derived from COF (C@COF) (part-1, 3.2 electrochemical studies).

3.4.1. Data Analysis of Co@COF-400

A CV with redox active peaks was obtained at variable scan rates from 2 to 2000 mV/s within the potential window from 0.0 to 0.8 mV (Figure 19A and 19B). Which indicates that the potential of this Co@COF derived carbon material to use it as Pseudocapacitor in acidic medium. This pseudo activity comes from Co nps which is doped in COF. The GCD charge-discharge profiles at variable current density appeared as symmetrically deformed triangular shape, which implied pseudo-capacitor behavior and ideal charge storage activity with good reversibility of the electrode material during the charge-discharge cycles (Figure 19C). This GCD profile shows gradual decrease of charge-discharge time with the increase of current density. Potentiostatic impedance analysis in this three-electrode system shows a very less charge transfer resistance as compared to the C@COF because the Cobalt which is doped will increase the conductivity (Figure 19D).

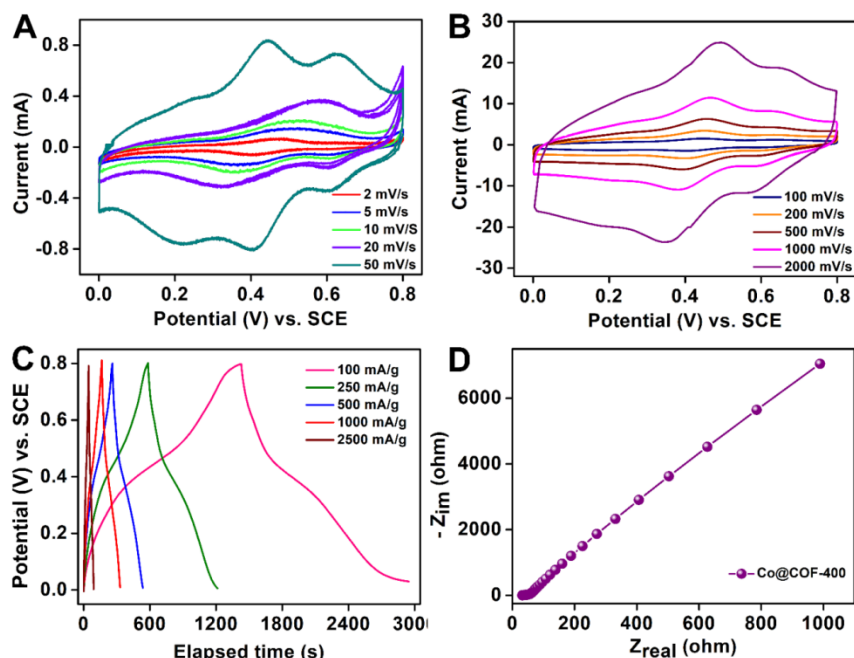


Figure 19: (A) and (B) Cyclic Voltammogram of Co@COF-400 from low to high the scan rates

in 1(M) H_2SO_4 electrolyte. **(C)** Galvanostatic Charge –Discharge profile of Co@COF-400 at different current densities. **(D)** Nyquist plot of Co@COF-400.

3.4.2. Data Analysis of Co@COF-750

A rectangular type CV without any redox-active peak was obtained at high scan rates from 100 to 2000 mV/s within the potential window from 0.0 to 0.8 mV/s. But a slight deformation of the shape of the CV occurs mainly in low potential at very low scan rates. (Figure 20A and 20B). Which indicates the possibility of this Co@COF (pyrolised at 750 °C) derived carbon material to use as supercapacitor in acidic medium. The GCD charge-discharge profiles appeared as equilateral triangle shapes, implied EDLC behavior and ideal charge storage activity with good reversibility of the electrode material in different scan rates (Figure 20C). Potentiostatic impedance analysis in this three-electrode system shows a very less charge transfer resistance.

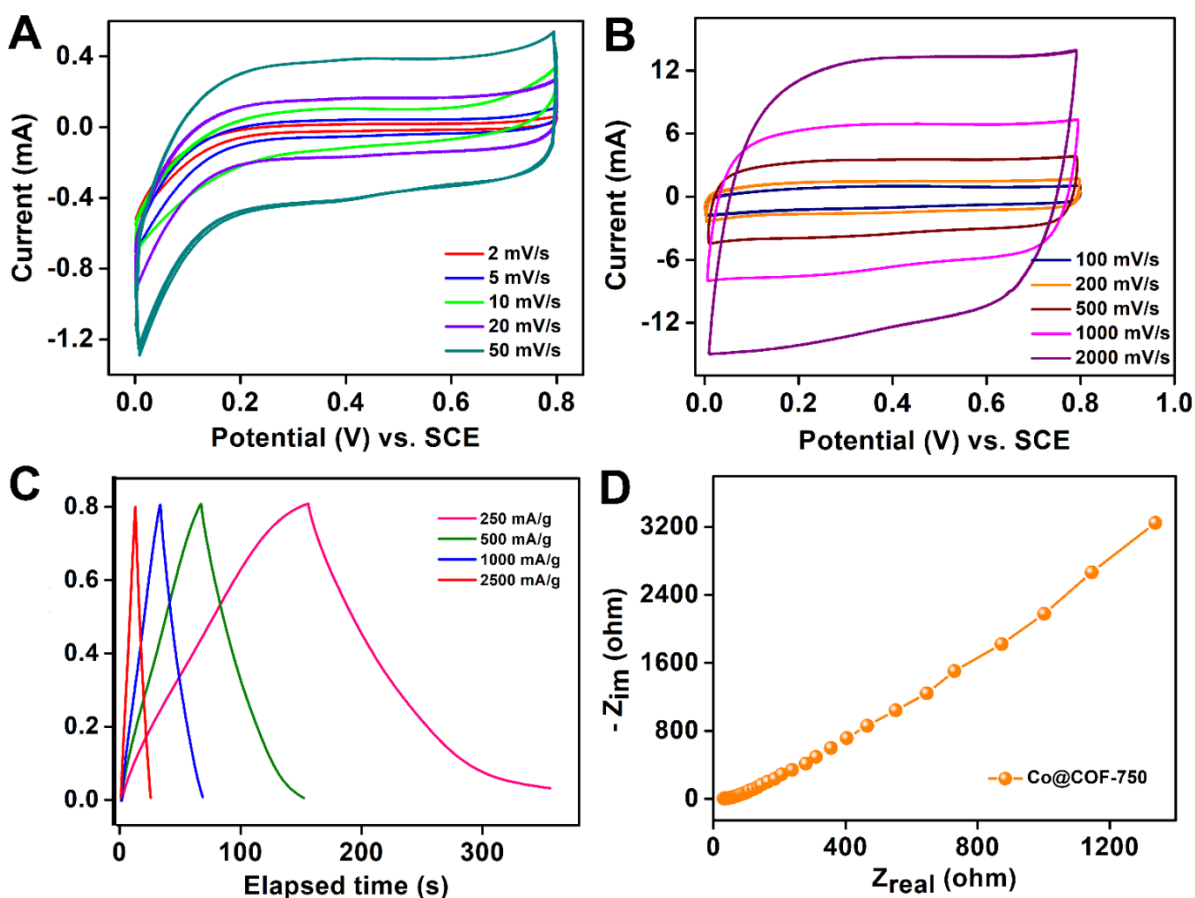


Figure 20: **(A)** and **(B)** Cyclic Voltammogram of Co@COF-750 from low to high the scan rates in 1(M) H_2SO_4 electrolyte. **(C)** Galvanostatic Charge–Discharge profile of Co@COF-750 at different current densities. **(D)** Nyquist plot of Co@COF-750.

3.4.3. Data Analysis

The comparison CV plot of Co@COF-400 and Co@COF-750 at 250 mV/s scan rate clearly shows the significant difference of capacitive nature between those two samples (Figure 21A & 21B). Where Co@COF-400 acts as pseudo-capacitor in acidic medium due to presence of reversible redox activity and Co@COF-750 acts as proper supercapacitor without having any redox reactions of the H⁺ with Co nps doped COF. For further confirmation CVs in very low to high scan rate were carried out for both Co@COF-400 and Co@COF-750. Which again indicates the presence of two prominent redox active peaks in case of Co@COF-400 even in very high (2 V/s) as well as in very low (2 mV/s) scan rate (Figure 19A & 19B). Whereas no such redox behavior was observed in case of Co@COF-750 even in very low scan rate of 2 mV/s (Figure 20A & 20B). This ambiguity can be explained as when the composite is pyrolysed at 750 °C the cobalt particles grow larger in size and are wrapped inside the carbon derived from COF. So, the H⁺ can't access the Co nps embedded into the carbon matrix to show redox activity.

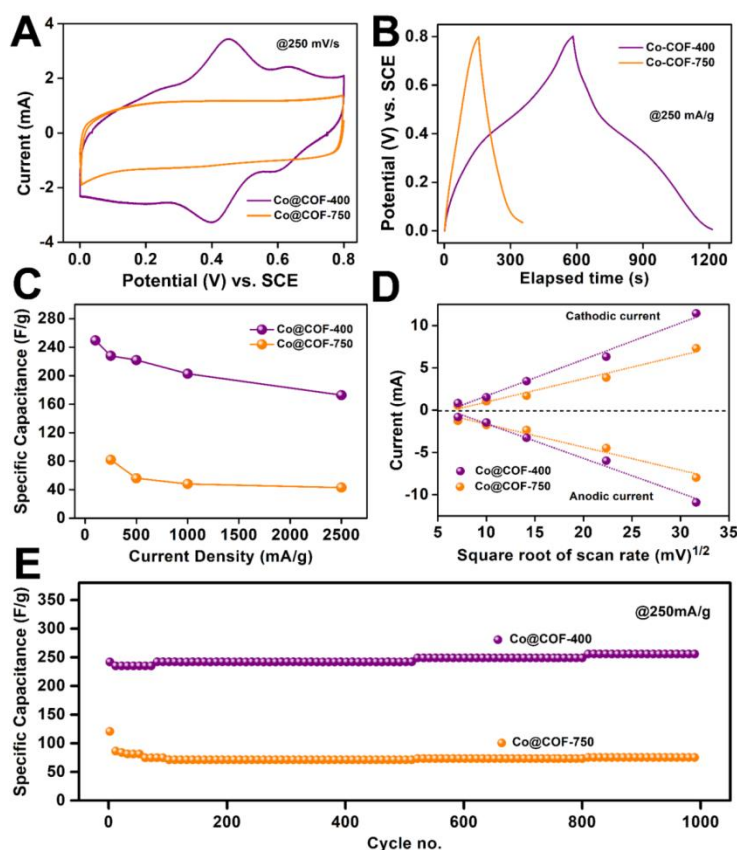


Figure 21: (A) Cyclic Voltammogram of Co@COF-400 and Co@COF-750 at 250 mV/s. (B) Galvanostatic Charge-Discharge (GCD) profile of Co@COF-400 and Co@COF-750 at 250 mA/g (C) Specific Capacitance variation with the change of current densities of Co@COF-400 and Co@COF-750. (D) A linear Fit of anodic peak current and cathodic peak current Vs Square Root of Scan Rate of Co@COF-400 and Co@COF-750. (E) Specific Capacitance retention after 1000 cycles Charge-discharge.

The shapes of GCD plots @250 mA/g current density are quite different for pseudo-capacitive Co@COF-400 and for super-capacitive Co@COF-750. The charging-discharging time is faster in Co@CoF-750 as compared to Co@COF-400. This infers that Co@COF-400 is able to store more charges. (Figure 21C). So, the specific capacitance is obtained for Co@COF-400 is higher i.e. 250 F/g at 100 mA/g and for Co@COF-750 that is only 80 F/g at 100 mA/g. The very low Specific capacitance of Co@COF-750 can be attributed to the fact of presence of negligible surface area to store H⁺ ion. Whereas the Co@COF-400 having comparable surface area to C@COF (Figure 14) had shown 226 F/g at 100 mA/g. For both the pyrolysed Co@COF samples, the drop-down in specific capacitance is lesser with the increase of the current density (Figure 19C). This is probably because of higher electronic conductivity of pyrolysed Co@COFs over C@COF (Figure 19D & 20D). However, 99% capacitance retention were achieved in both the cases at 250 mA/g current density even after 1000 cycles charging and discharging (Figure 19E). The mechanism of charge storage can follow either charge transfer or mass transfer or both. This can be established from a plot of the peak current vs. square root of the scan rate. The cathodic and anodic peak current of Co@COF-400 and Co@COF-750 increases linearly with the square root of scan rate demonstrating that the fast kinetics associated with H⁺ ion diffusion in the bulk materials (Figure 21D).

Material	Surface area (m ² /g)	Capacitance value (F/g)	Reduction of capacitance from (250 mA/g to 1 A/g) (%)	Retention of the capacitance after cycling (%)
C@COF	505	224	42	99
Co@COF-400	480	250	11	99
Co@COF-750	79	80	30	99

Table 1: For better understanding the above comparison table has been made.

4.0. CONCLUSION

We have successfully synthesized the COF (which is already reported in our lab) and Cobalt nps doped COF (Co@COF). This COF and Co@COF is pyrolysis at different temperatures (COF at 750^o C and Co@COF at 400^o C and 750^o C). And we have done some characterizations by different techniques (such as PXRD, TGA, IR, FE-SEM, Adsorption isotherms, and EDS). We have also done electrochemical studies for these samples. Among all samples the Co@COF-400 showed the best results than the other samples (such as C@COF and Co@COF-750). Among all samples the surface area of the C@COF (BET-505 m²/g and Langmuir-606 m²/g) is more compared to Co@COF-400(BET-480 m²/g and Langmuir-632 m²/g) and Co@COF-750 (BET-79 m²/g and Langmuir-108 m²/g) because Cobalt Nanoparticles are embedded into the pore of the COF these occupy some amount of the surface area. The capacitance value in acidic medium for C@COF is almost comparable to the Co@COF-400. Because capacitance is only a surface active phenomenon which does not vary much as the C@COF and Co@COF provides similar surface area. But interestingly slightly increased value of the capacitance in low current density as well as higher current density was achieved by introducing Co-nps into COF. This is due to the redox active nature of pseudo capacitive Co@COF-400 and due to its enhanced electronic

conductivity. In high scan rate which is able to propagate the electron very quickly through the comparatively higher conducting material. Whereas burning the Co@COF in higher temperature (750 °C) reduces the active surface for H⁺ storage. And capacitance reduces a lot.

5.0. REFERENCES

- (1) Waller, P. J.; Gándara, F.; Yaghi, O. M. Chemistry of Covalent Organic Frameworks. *Acc. Chem. Res.* **2015**, *48*, 3053.
- (2) Pachfule, P.; Kandambeth, S.; Díaz, D. D.; Banerjee, R. Highly Stable Covalent Organic Framework–Au Nanoparticles Hybrids for Enhanced Activity for Nitrophenol Reduction. *Chem. Commun.* **2014**, *50*, 3169.
- (3) Segura, J. L.; Mancheno, M. J.; Zamora, F. Covalent Organic Frameworks Based on Schiff-base Chemistry: Synthesis, Properties and Potential Applications. *Chem. Soc. Rev.* **2016**, *45*, 5635.
- (4) Mendoza, J. L.; Pascal, T. A.; Goddard, W. A.; Design of Covalent Organic Frameworks for Methane Storage, *J. Phys. Chem. A* **2011**, *115*, 13852–13857.
- (5) Sharma, A.; Malani, A. A.; Medhekar, N. V.; Babarao, R.; CO₂ adsorption and separation in covalent organic frameworks with interlayer slipping, *CrystEngComm*, **2017**, *19*, 6950– 6963.
- (6) Ding, S. Y.; Gao, J.; Wang, Q.; Zhang, Y.; Song, W. G.; Su, C. Y.; Wang, W. Construction of Covalent Organic Framework for Catalysis: Pd/COF-LZU1 in Suzuki–Miyaura Coupling Reaction. *J. Am. Chem. Soc.* **2011**, *133*, 19816.
- (7) Mullangi, D.; Dhavale, V.; Shalini, S.; Nandi, S.; Collins, S.; Woo, T.; Kurungot, S.; Vaidhyanathan, R. Low-Overpotential Electrocatalytic Water Splitting with Noble-Metal- Free Nanoparticles Supported in a sp³ N-Rich Flexible COF. *Adv. Energy Mater.* **2016**, *6*, 1600110.
- (8) Xu, Q.; Tang, Y.; Zhai, L.; Chena, Q.; Jiang, D. Pyrolysis of Covalent Organic Frameworks: A General Strategy for Template Converting Conventional Skeletons into Conducting Microporous Carbons for High-performance Energy Storage. *Chem. Commun.* **2017**, *53*, 11690-11693.

-
- (9) Huang, Y.-B.; Pachfule, P.; Sun, J.-K.; Xu, Q. From Covalent-organic Frameworks to Hierarchically Porous B-doped Carbons: A Moltensalt Approach. *J. Mater. Chem. A*. **2016**, *4*, 4273-4279.
- (10) Xu, Q.; Tang, Y.; Zhang, X.; Oshima, Y.; Chen, Q.; Jiang, D. Template Conversion of Covalent Organic Frameworks into 2D Conducting Nanocarbons for Catalyzing Oxygen Reduction Reaction. *Adv. Mater.* **2018**, 1706330.
- (11) Chen, L.; Zhang, L.; Chen, Z.; Liu, H.; Luque, R.; Li, Y. A Covalent Organic Framework-based Route to the in Situ Encapsulation of Metal Nanoparticles in N-rich Hollow Carbon Spheres. *Chem. Sci.* **2016**, *7*, 6015-6020.
- (12) Bhanja, P.; Bhunja, k.; Das, S. K.; Pradhan, D.; Kimura, R.; Hijikata, Y.; Irle, S.; Bhaumik, A. A New Triazine-Based Covalent Organic Framework for High-Performance Capacitive Energy Storage. *ChemSusChem*. **2017**, *10*, 921-929.
- (13) Cheng, J. P.; Chen, X.; Wu, J.-S.; Liu, F.; Zhang, X. B.; David, V. P. Porous cobalt oxides with tunable hierarchical morphologies for supercapacitor electrodes. *CrystEngComm*. **2012**, *14*, 6702–6709.
- (14) Mullangi, D.; Nandi, S.; Shalini, S.; Sreedhala, S.; Vinod, C. P.; Vaidhyanathan, R. Pd loaded amphiphilic COF as catalyst for multi-fold Heck reactions, C-C couplings and CO oxidation. *Sci. rep.* **2015**, *5*, 10876.
- (15) Mullangi, D.; Chakraborty, D.; Pradeep, A.; Koshti, V.; Vinod, C.P.; Panja, S. P.; Nair, S.; Vaidhyanathan, R.; *Small*. **2018**, 1801233.